World Scientific
www.worldscientific.com

JAPAN SOCIETY OF CIVIL ENGINEERS
COASTAL ENGINEERING COMMITTEE

Coastal Engineering Journal, Vol. 45, No. 3 (2003) 439–469

SIMULATION OF WAVES AT DUCK (NORTH CAROLINA) USING TWO NUMERICAL MODELS

KHALID ZUBIER
Faculty of Marine Sciences, King Abdulaziz University,
P. O. Box 80207, Jeddah 21589, Saudi Arabia

VIJAY PANCHANG*
Department of Maritime Systems Engineering, Texas A&M University,
200 Seawolf Parkway, Galveston, TX 77553, USA
panchanv@tamug.tamu.edu

ZEKI DEMIRBILEK
US Army Engineer R&D Center, Coastal and Hydraulics Laboratory,
Vicksburg, MS 39180-6199, USA
Zeki.Demirbilek@erdc.usace.army.mil

Revised 19 April 2002
Revised 14 May 2003

Two wave transformation models, SWAN and CGWAVE, are used to simulate wave conditions at the Field Research Facility, Duck (North Carolina). The motivation is to examine how well these models reproduce observations and to determine the level of consistency between the two models. Stationary wave conditions pertaining to three different storm-induced bathymetric representations are modelled. It was found that SWAN and CGWAVE reproduced the observed wave behavior to a large extent, but CGWAVE results tended to be somewhat smaller than the SWAN results and the measurements. The differences were attributed to wave-wave interactions and breaking. Otherwise the models showed a high level of consistency. SWAN and CGWAVE were also used to explore other mechanisms reported in recent literature; the results were either consistent with some observations (in the case of the nonlinear mechanisms) or they shed more light on others (in case of the role of the research pier legs).

Keywords: Waves; model; SWAN; CGWAVE; FRF; pier; pilings; validation.

*Corresponding author.

1. Introduction

In the United States and Europe, the development of ocean observing systems is receiving increased attention. These systems are intended to procure and disseminate data regarding various ocean parameters to user communities at regular intervals (see special issues of *Coastal Engineering* (Sep. 2000, "Operational Oceanography in Coastal Waters") and *Oceanography* [v. 13, 1, 2000)]. Mathematical modeling methods constitute an integral component of such systems. In the context of waves, models like WAM [Komen *et al.* (1995)] and WAVEWATCH [Tolman (1989)] are now routinely operational and produce ongoing forecasts for much of the global oceans. However, the resolution used in these systems is too coarse for obtaining reliable wave information in coastal regions (for example, around the US, the National Weather Service uses grids varying between 0.5 and 1.25 degrees) and the models are not intended to handle complex geometric features and the resulting wave-scattering effects such as reflections, diffraction, etc. that may be important in nearshore areas.

A suite of models may therefore be needed to perform operational simulations in coastal regions and one component may consist of the local use of specialized models in the intermediate region between the grid points of the outer-ocean WAM or WAVEWATCH operations and the very nearshore areas. This intermediate domain, which may be of the order of about 50 km, may experience wave growth due to wind and call for the use of energy balance models. Much closer to the coast (e.g. in regions like harbors) where wave transformation is governed by the domain geometry, it may be necessary to model the wave motion itself using phase-resolving models (as opposed to modeling merely the energy transport). Panchang *et al.* (1998) provide a review of coastal wave modeling tools that have been developed in the last two decades.

One difficulty with operational modeling of waves in coastal areas pertains to the reliability of the predictions. For the outer ocean wave models, the length scale of the wind-induced changes is large and the combination of the available buoy and satellite data in the domain are generally sufficient for model validation. In coastal areas, however, spatial variability induced by geometric irregularities can be greater and more complex. Yet, most model domains will have little or no data for validation/calibration. Satellite data close to the coast are not reliable [Siddabathula and Panchang (1996)] and buoys, if at all present, are too localized to provide a proper representation of the complete wave scattering problem. ([Zhao *et al.* (2001)] discuss the effects of undersampling while making model-data comparisons.) Even when data are available, they would most likely contain the effects of physical mechanisms not modelled. It is obvious that unlike regional tidal/circulation models, it is difficult to validate or calibrate a regional coastal wave model used in an ocean observing system. Based on their examination of several coastal engineering models, Thieler *et al.* (2000) complain that assumptions and predictions associated with many currently-used models are either poor or totally invalid. In order to invest

faith in the predictions, it is therefore necessary to validate the models whenever the opportunity exists and, if satisfactory results are obtained, to apply them at other desired sites in the hope that the predictions are reliable. It is also necessary to compare the results of models based on completely different formulations and to explore their ability to simulate the role of various processes. The purpose of this paper is to examine the performance of two models, the energy balance model SWAN [Booij *et al.* (1999)] and the phase-resolving model CGWAVE (Demirbilek and Panchang, 1998; Panchang and Demirbilek, 2001, 2002) in a field application. The domain of interest, the Field Research Facility (FRF) at Duck (North Carolina, USA), contains a greater number of measurements than are normally available. The use of the two models, in which some components of the wave physics are similar and others are different, allows one to isolate these components and to examine their effects.

The research presented in this paper consists of three parts. First, a comparison is made, in a quantitative sense, between the results of the two models themselves and between the model results and the observations at two FRF wave gauges. In this part we also try to quantify the significance of some of the physical mechanisms that the models account for. In the second part, the qualitative performance of the two models is examined by comparing the model results for the three storm events with some field observations made by other researchers at FRF during different time periods. Finally, we use the results of the two models in a quantitative-qualitative sense to investigate the effect of the piles of the FRF research pier on obliquely approaching waves as they pass under the pier during an event that has been studied by other researchers.

The layout of this paper is as follows. In Sec. 2, a brief description of the two models is given. This is followed, in Sec. 3, by some details about the study area and the modeling schemes. The results are discussed in Sec. 4. Concluding remarks are given in Sec. 5.

2. Description of Models

The model CGWAVE [Demirbilek and Panchang (1998)] is a two-dimensional model developed at the University of Maine (USA). It is based on the following extension of the "combined refraction-diffraction" equation:

$$\nabla \cdot (CC_g \nabla \Phi) + (k^2 CC_g + i\sigma w + iC_g \sigma\gamma)\Phi = 0 \tag{1}$$

where, for a given wave frequency σ, $\Phi(x, y)$ is the wave potential from which the wave height and phase may be estimated, C is the wave velocity, C_g is the group velocity, k is the wave number, w is a bottom friction factor, and γ is the wave breaking parameter. This equation is applicable to both long and short waves and hence finds wide application. (See Mei (1983) and Panchang *et al.* (1999) for details.) The mild-slope assumption associated with (1) requires that for local depth d,

($|\nabla d|/kd$) << 1, a criterion that is usually met in practice. Being elliptic, the equation represents a boundary value problem, which can accommodate internal non-homogeneities and boundaries. It hence forms a well-accepted basis for performing wave simulations in regions with arbitrarily-shaped (manmade or natural) boundaries and arbitrary depth variations without limitations on the angle of wave incidence or the degree and direction of wave reflection and scattering that can be modelled. In essence, it represents the complete two-dimensional wave-scattering problem for the non-homogeneous Helmholtz equation. Irregular wave conditions may be simulated using (1) by superposition of monochromatic simulations (e.g. Chawla *et al.*, 1998; Panchang *et al.*, 1990; Zhao *et al.*, 2001).

CGWAVE uses a triangular finite-element formulation with grid sizes varying throughout the domain based on the local wavelength. The model allows one to specify the desired reflection properties along the coastline and other internal boundaries via a Robbins' type boundary condition ($\delta\Phi/\delta n = \alpha\Phi$, where α is related to the reflection coefficient). The model also uses a semi-circle (as an open boundary) to separate the model domain from the outer sea. Examples of typical CGWAVE model domains are described later (e.g. Fig. 3). The input conditions are provided at the offshore ends of two one-dimensional cross-shore sections. (In practice, the input condition is known at the end of one of the transects. The condition at the offshore end of the other transect is obtained by appropriate phase translation.) A combination of the incident and reflected waves is computed along these transects using a one-dimensional version of (1); this partial solution is then mapped on to the semicircle to force the two-dimensional model. The remainder of the solution on the boundary consists of a scattered wave that emanates from within the domain; this component is allowed to radiate out through the use of an impedance boundary condition. (For detailed descriptions, see Panchang *et al.*, 2000; Zhao *et al.*, 2001; and Panchang and Demirbilek, 2001).

The model SWAN is a third generation wave model developed at the Technical University of Delft in the Netherlands (Booij *et al.*, 1999; Ris *et al.*, 1998; and Ris *et al.*, 1999). The model is based on the following spectral action balance equation:

$$\frac{\partial}{\partial t}N + \frac{\partial}{\partial x}c_x N + \frac{\partial}{\partial y}c_y N + \frac{\partial}{\partial \sigma}c_\sigma N + \frac{\partial}{\partial \theta}c_\theta N = \frac{S}{\sigma} \tag{2}$$

where N is the action density (= spectral energy/σ), θ is the wave direction, and c_x and c_y are components of the wave propagation velocity. The first term on the left hand side of (2) represents the rate of change of action in time and the second and the third terms represent the propagation of action in the (x, y) space. The fourth and fifth terms represent, respectively, the frequency shift and refraction induced by depth and currents. The source/sink term (S) on the right hand side of (2) represents the effects of generation, dissipation (due to breaking, bottom-friction, and whitecapping), and nonlinear wave-wave interactions. In the present study, we

have used the following steady state version of (2):

$$\frac{\partial}{\partial x}c_x N + \frac{\partial}{\partial y}c_y N + \frac{\partial}{\partial \theta}c_\theta N = \frac{S}{\sigma} \tag{3}$$

where it has been assumed that over the length scales of interest, the propagation times are small enough so that unsteady effects may be ignored (e.g. Booij *et al.*, 1996). This makes the model compatible with CGWAVE, which is a quasi-steady (time-harmonic) model. Further, in an ocean observing system, computational efficiency may demand that these models be run in the steady mode at frequent time intervals (say 3 hours), forced by the output from the outer ocean WAM/WAVEWATCH simulations. (The domains for coastal models such as CGWAVE often involve about half a million nodes, making unsteady or more frequent simulations impractical.) The effects of currents are also not considered in the present study ($c_\sigma = 0$). The governing equation is solved using finite differences for a spectral or parametric input specified along the boundaries (Booij *et al.*, 1999; Ris, 1997).

SWAN can use either a rectilinear or curvilinear computational grids with a uniform grid size in either case. Although, unlike CGWAVE, the grid size in SWAN is independent of the water depth, it should be small enough to resolve the changes in bathymetric, wind, and wave fields. The boundaries of SWAN computational grid are either land or water. The land boundary absorbs all incoming waves (reflection is not accounted for). Input wave conditions can be defined along the water boundaries if observations or results from another model run are available (e.g. Rogers *et al.*, 2002). However, if wave input conditions are only defined along one of the three water boundaries then along the other two, waves cannot enter the domain but can only leave freely. This assumption is obviously a source of error and therefore it is necessary to select such lateral boundaries to be sufficiently far away from where reliable computations are needed in order to minimize the lateral boundary effect on the model results at that area of interest.

The major differences in the two models lie in the fact that (1) is based on the Laplace equation and hence models the wave motion, while (2) models the transport of energy. As a consequence, the effects of wind generation cannot be included in the former, while the effects of reflection and diffraction cannot be included in the latter. [*Ad hoc* attempts to remedy these limitations have been described by Booij *et al.*, (1997) and Pearce and Panchang (1985).] Thus, CGWAVE is not appropriate for cases where wave generation by wind is significant, and simulation with SWAN in areas with complex bathymetry, around islands or structures, and in semi-closed areas such as harbors and inlets may be difficult. (It is noted that despite such limitations, Bondzie and Panchang (1993) found that the wave model HISWA (the predecessor of SWAN) provided reasonable simulations in one test involving complex caustic-causing bathymetry.) The grid resolution is also generally different: phase resolving models require a resolution that is a fraction of the wavelength, while energy

balance model grids can be much larger. Other differences also exist; these are due to the fact that (unlike SWAN) the version of CGWAVE used in this study does not include whitecapping and non-linear wave-wave interactions. However, such limitations can be remedied in the future. [To elucidate, whitecapping may be regarded as a modification to γ, and nonlinear resonant interactions can be included in the governing equation (1) following Tang and Oullet (1997) and Kaihatu and Kirby (1995).] In general, however, the modeller does not *a priori* know how significant these mechanisms are in a given application. If the physics are similar, the models should produce similar results despite the difference in their genesis.

3. Study Area and Modeling Details

The Field Research Facility (FRF) is a unique facility that is operated by the US Army Corps of Engineers to study coastal processes and has been internationally recognized for its coastal studies. FRF (Fig. 1), which faces the North Atlantic Ocean, is located near the town of Duck (North Carolina) and is subject to frequent storms and hurricanes. A nearshore sand bar, which often forms during the moderate phase of a storm, migrates offshore as the storm intensifies. The bottom slope at the FRF varies on average between 1:20 offshore of the sand bar and a steep 1:5 near the beach. The

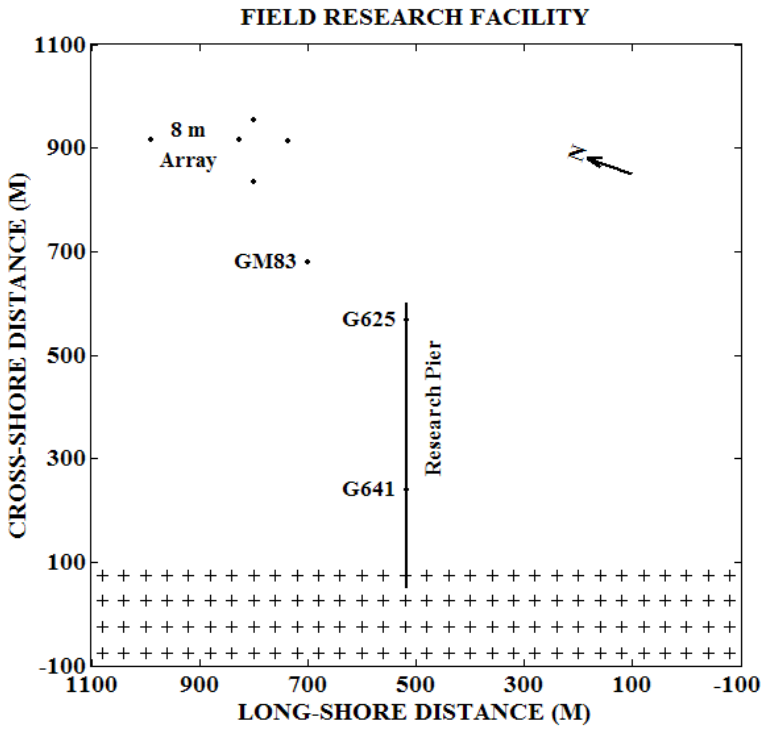

Fig. 1. Plan view of the Field Research Facility (FRF), showing the locations of instruments. + represents land areas.

FRF research pier extends 561 m offshore and is supported by 108 concrete-filled steel piles, each with diameter of approximately 0.85 metres. Under the pier, a permanent bathymetric trough exists, but its shape and depth changes with the wave conditions. Specialized equipment and instruments constantly monitor the changing bathymetry, winds, waves, tides, and currents. All measurements made at the FRF can be downloaded from the FRF web-site (http://www.frf.usace.army.mil).

Simulations were performed for wave conditions observed during three different storm events that occurred at FRF (Table 1 and later in Fig. 4). These events, which occurred in 1994, 1996, and 1998, were selected as a consequence of both the availability of the data (mainly bathymetric) and the severity of the storm conditions. Data pertaining to the bathymetry, waves, winds, and sea levels were used in this study. During the peak of the storms, the conditions were largely steady, as illustrated in Fig. 2, which shows wind measurements collected at the offshore end of the research pier and wave measurements collected by one of the 8 m array gauges.

The changing bathymetry at FRF is monitored using the "Coastal Research Amphibious Buggy" which records, at irregular intervals, bathymetric data along cross-shore sections separated by about 40 metres. On each cross-shore transect, measurements are made at a spacing of 0.5–0.75 meters. Temporal changes in the bathymetry at FRF are quite significant (Howd and Birkemeier, 1987) due to the wave action during storm events. For instance, Gallagher *et al.* (1998) observed a 130 m movement of the crest of the nearshore sand bar during a two-month period in the fall of 1994 that included three storms. As a consequence of such changes, each of the three cases investigated in this study is unique and requires a different model grid. Further difficulties arise due to the fact that SWAN and CGWAVE use

Table 1. Observed wave conditions at FRF during three storm events. Hs, Tp, Dp, and Ds represent significant wave height, peak wave period, peak wave direction and averaged wave directional spreading respectively. All directions are from true north. The underlined values at the 8-m array location also represent the spectral parameters of the input conditions used for simulating each storm event.

Data Time	Location	Hs (m)	Tp (sec)	Dp (deg)	Ds (deg)
Nov. 18, 1994	8-m Array	5.140	13.563	80.0	21.4
04:00–06:16	Gauge625	3.135	14.238		
	Gauge641	1.442	14.745		
Sep. 06, 1996	8-m Array	3.270	8.866	94.0	20.9
01:00–03:16	Gauge625	2.708	8.891		
	Gauge641	1.628	8.790		
May 13, 1998	8-m Array	3.280	11.976	64.0	20.6
13:00–15:16	Gauge625	2.673	12.434		
	Gauge641	1.276	12.019		

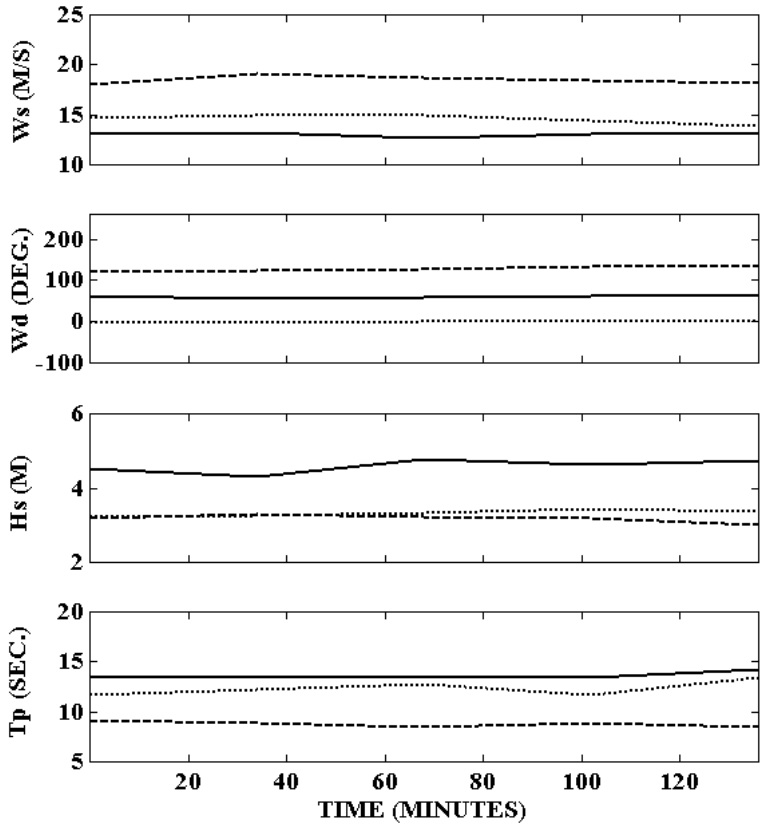

Fig. 2. Wind speed (Ws), wind direction (Wd), significant wave height (Hs), and peak wave period (Tp) data for the time periods investigated (8192 seconds) for the three storm events, 1994 (solid lines), 1996 (dashed lines) and 1998 (dotted lines).

different kinds of grids, so that two different model grids must be generated for each storm event.

For SWAN, a rectilinear computational grid is generated with a grid size of 8 m $\times$ 8 m for each case. The three different computational grids extend for 800 m in the cross-shore direction between y = 100 m and 900 m (Fig. 1). In the long-shore direction, the computational domains were extended on each side sufficiently (by about 200 m) beyond our area of interest, which is between 100 m and 900 m long-shore coordinate, in order to minimize any effect of the lateral boundaries. (Sensitivity analyses were also performed by using even larger domains to check that the area of interest was unaffected by possible spurious boundary effects). The generated computational grids contained 13,750, 15,000, and 14,300 grids for 1994, 1996 and 1998 events respectively. In SWAN, the coastline absorbs all the incoming waves.

For CGWAVE, grid-generation is more complicated since the resolution is based on the wavelength, which is a function of water depth. For each case, a mesh of

non-equal size triangular finite elements was generated for the domain with a semi-circular open boundary using the grid-generation package contained in the "Surface-Water Modeling System" [Zundell *et al.* (1998)]. The alongshore extents of the three CGWAVE domains were almost equal to those used in SWAN domains. For each event, a model grid was generated such that there were at least 10 nodes per wavelength, and resulted in 72,440, 88,629, and 76,180 finite elements for the three cases. Since small features can be more readily accommodated with finite elements, the pilings of the FRF research pier were included in the CGWAVE grid (but not in the SWAN simulations). This was done because recently Elgar *et al.* (2001) have investigated the effects of the research pier on the data collected at FRF. The 76 research pier pilings that were accommodated were considered to be a fully reflective. The coastline was assumed to be a fully absorbing boundary.

It must be noted here that since all non-homogeneities are enclosed in domains of different shapes for the SWAN and CGWAVE simulations, the modelled scenarios are similar but not identical. An example of the two different domains is shown in Fig. 3 for the bathymetry used for the 1998 storm event. Because of differences in grid resolution, the bathymetric representation in the two model domains is somewhat different.

Another feature in which the simulations differ pertains to the open boundary conditions used by each model. Input conditions to SWAN are defined along the offshore boundary of the rectangular domain (i.e. at $y = 900$ m). For CGWAVE, the input conditions are provided at the offshore ends of the two one-dimensional cross-shore sections (dotted lines in Fig. 3) that also extends to $y = 900$ m. The input wave conditions were based on frequency-direction spectra, Fig. 4, obtained from the 9-element linear array of pressure gauges located on the 8 m depth contour about 900 m offshore (Fig. 1). Each spectrum is based on an 8192-second time-series of data collected at 2 Hz. Each spectrum consists of 29 frequency components between 0.04443 Hz and 0.31787 Hz with frequency resolution of about 0.00977 Hz and 90 directional components distributed into 45 directional bins on either side of the research pier with a resolution of 2 degrees. The resulting 2610 spectral components were used to force SWAN. However, the much larger number of grids in CGWAVE simulations precluded the inclusion of such a large number of components. The spectral discretization provided to CGWAVE was based on eliminating components containing energy less than a prespecified threshold (0.09% of the total energy) and enhancing the energy content of the remaining components to reproduce the desired incident wave conditions.

Uniform winds were assumed over the SWAN domain based on averaged wind measurements at the end of the FRF research pier. Tidal measurements, collected by a tide gauge located at the offshore end of the research pier, were also used to adjust the water depths in the domains. The observed wave conditions at the two gauges

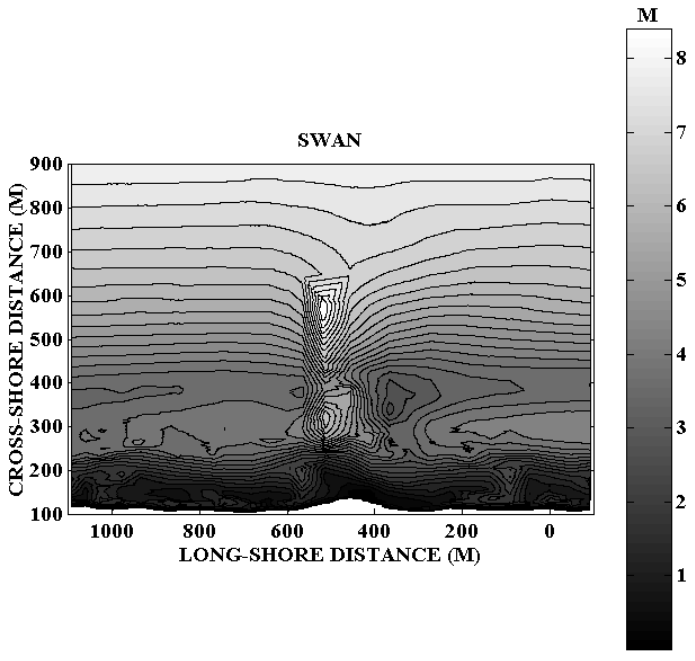

(Top Panel)

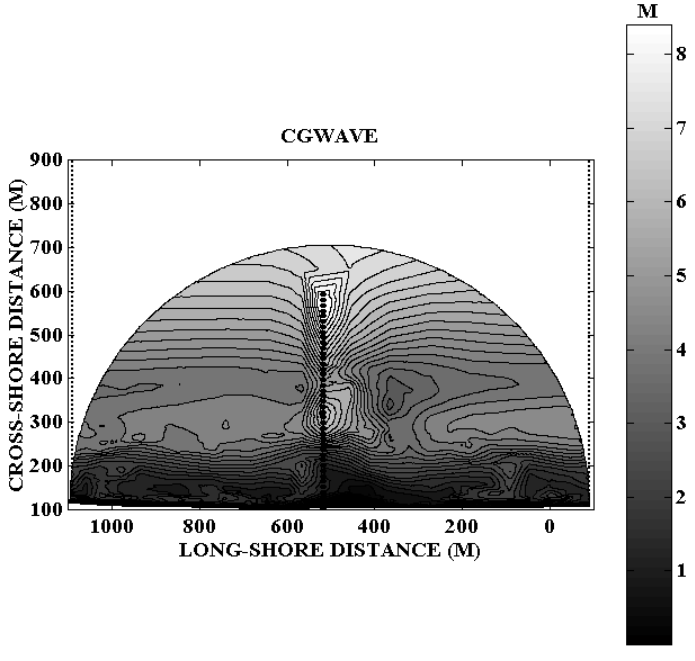

(Bottom Panel)

Fig. 3. Model domains and bathymetry for SWAN (top panel) and CGWAVE (bottom panel) simulations of the May 1998 storm event.

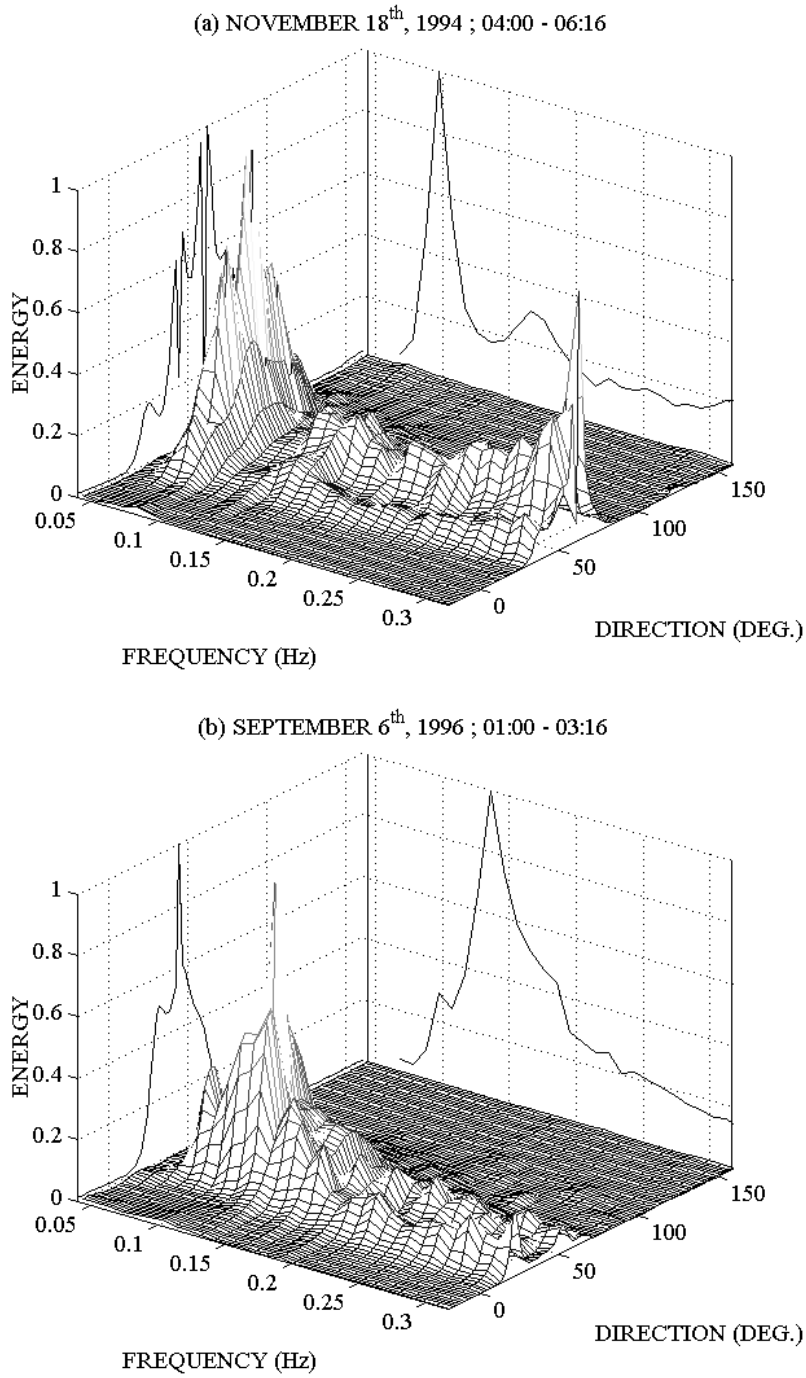

Fig. 4. Input directional wave spectra used to force SWAN (shown normalized) for the three simulations (a) 19994, (b) 1996 and (c) 1998. Left wall, normalized 1-d directional spectrum for peak frequency; facing wall, normalized 1-d frequency spectrum.

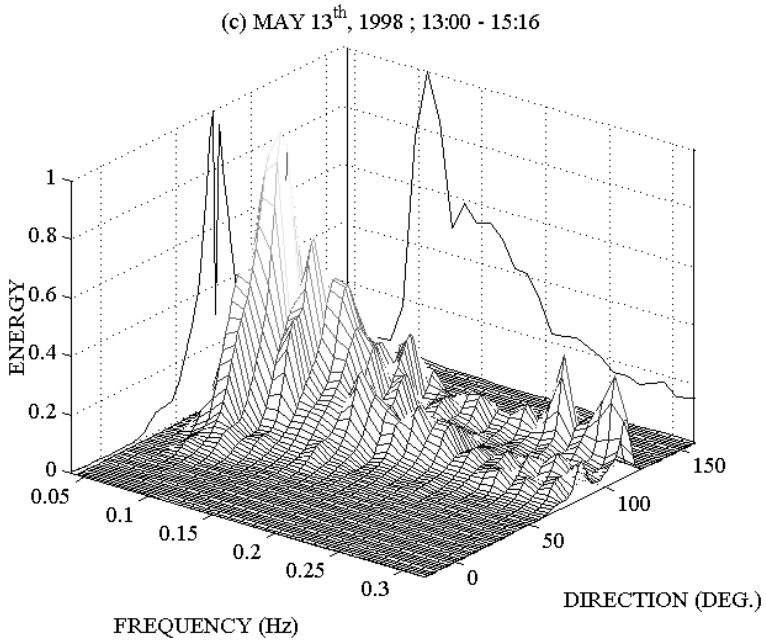

Fig. 4 (*Continued*)

located under the FRF research pier (denoted by "G641" and "G625" in Fig. 1) are compared to the model output to determine the quantitative performance of the two models. At these two gauges the wave conditions are measured every 34 minutes (based on a record of 4096 data points with a sampling frequency of 2 Hz); therefore, for each case a total of five measurements were averaged at each wave gauge.

The SWAN model runs were made using a personal computer equipped with an AMD Athlon 700 MHz processor and 256 megabytes of RAM. On average, a SWAN run takes about 1 hour. Spectral CGWAVE runs were made using a highly parallelized version of the code (described by Bova *et al.*, 2000) on the US Army Corps of Engineers' supercomputer. For non-breaking runs, a typical simulation for 400 spectral components using 50 processors takes about 3 minutes. However, when breaking is specified as a function of all spectral components (i.e. the significant wave height), the effect of the parallelization is diminished and a typical simulation requires about 20 hours.

4. Results and Discussion

The model results are presented and discussed in the following order. After a preliminary quality control examination of model performance, we describe quantitative and then qualitative aspects of the results based on the simulation of the three storm events. Then we provide a quantitative-qualitative study of the effect of the piles of FRF research pier on the waves.

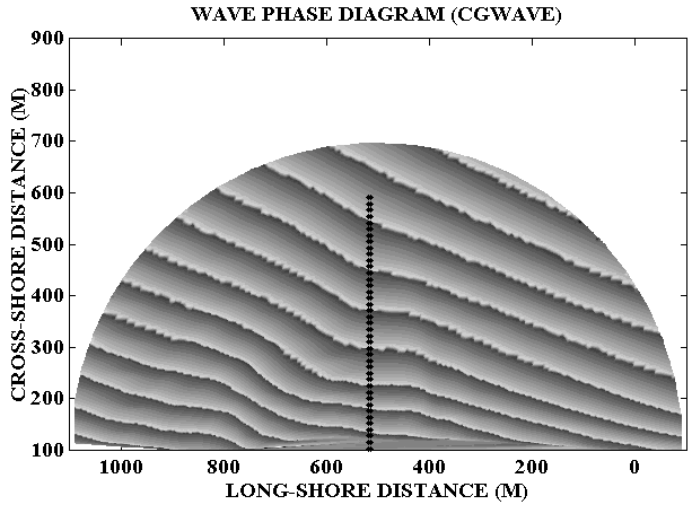

(Top Panel)

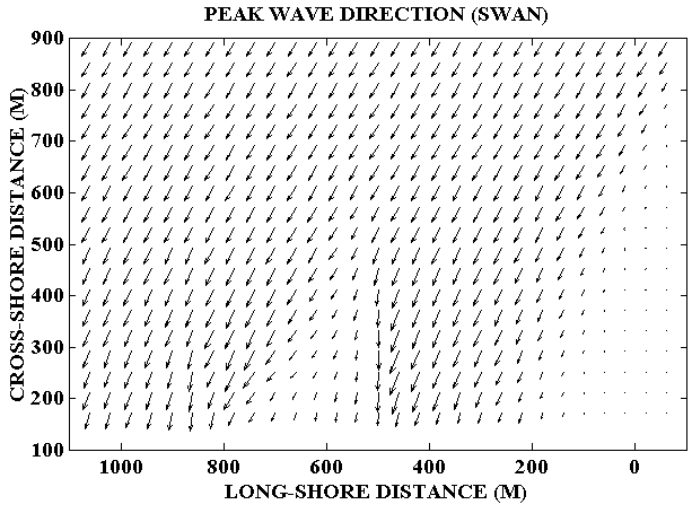

Bottom Panel)

Fig. 5. Phase diagram (top panel) produced by CGWAVE and peak wave directions (bottom panel) produced by SWAN for a monochromatic wave incident from 30 degrees to the right of the research pier with height = 1 m and peak period = 10.6 seconds. Length of arrows corresponds to magnitude of significant wave height (Hs).

Before the three storm events were simulated, the performance of the two numerical models was initially examined in a qualitative sense. This was done by simulating several cases with different monochromatic incident wave conditions. While this is not a problem with CGWAVE, SWAN does not really run in a monochromatic mode; a narrow-peaked spectrum was therefore provided as input. Figure 5 shows the results obtained for the 1996 bathymetry for an incident wave of height

= 1 m, period = 10.6 seconds, and angle of approach = 30 degrees to the right of the pier. The phase diagram (showing cosine of the phase) obtained from the CGWAVE simulation, Fig. 5 (top panel), shows the expected bending of the phase lines due to refraction across the bathymetry and the expected decrease in the wavelength in the shoreward direction. No spurious oscillations encountered in earlier models of this category (e.g. Thompson *et al.*, 1996) are seen. Peak wave directions obtained with SWAN, shown in Fig. 5 (bottom panel), also appear to be reasonable and orthogonal to the phase diagram shown in Fig. 5 (top panel). These and other tests indicated satisfactory performance. (Note that in these and other figures, the offshore extent of the two domains is different; even though this dimension is smaller for the CGWAVE domain, as noted earlier, the input waves are specified at the same location for both models (Fig. 3) by using the two 1-D sections to account for the effect beyond the offshore end of the semi-circular domain.)

4.1. *Quantitative Model Performance*

All simulations with SWAN have been made with the default formulations for wind generation, wave refraction, wave breaking, bottom friction, wave-wave interactions, and white-capping (Booij *et al.*, 1999). Initially, SWAN runs were made with all the physical mechanisms turned on ("all-on runs") for all 3 conditions. An example of the significant wave heights computed with SWAN is shown in Fig. 6 (top panel) for the 1998 simulation. The results at the gauge locations are given in Table 2 and Fig. 7 (top panel) for all three conditions. It may be seen that SWAN simulates

Table 2. SWAN-computed significant wave heights (Hs) and peak wave periods (Tp) for three storm events with different physics incorporated.

	Date:	Nov. 18, 1994		Sep. 06, 1996		May 13, 1998	
	Time:	04:00–06:16		01:00–03:16		13:00–15:16	
Physics	Gage #	Hs (m)	Tp (sec)	Hs (m)	Tp (sec)	Hs (m)	Tp (sec)
All On	625	3.143	13.529	2.717	8.536	2.692	12.530
	641	1.446	13.529	1.629	8.536	1.081	12.530
Wind Off	625	3.194	13.529	2.792	8.536	2.625	12.530
	641	1.414	13.529	1.597	8.536	1.034	12.530
Refrc. Off	625	3.338	13.529	2.820	8.536	2.790	12.530
	641	2.336	13.529	2.000	9.217	2.090	12.530
Break. Off	625	4.685	13.529	3.013	8.536	2.944	11.604
	641	3.077	13.529	2.635	8.536	1.958	11.604
Frict. Off	625	3.170	13.529	2.740	8.536	2.715	12.530
	641	1.463	13.529	1.656	8.536	1.095	12.530
Triad Off	625	3.179	13.529	2.851	8.536	2.649	11.604
	641	1.381	13.529	1.538	8.536	1.006	11.604
Wtcap. Off	625	3.145	13.529	2.723	8.536	2.694	12.530
	641	1.448	13.529	1.630	8.536	1.082	12.530

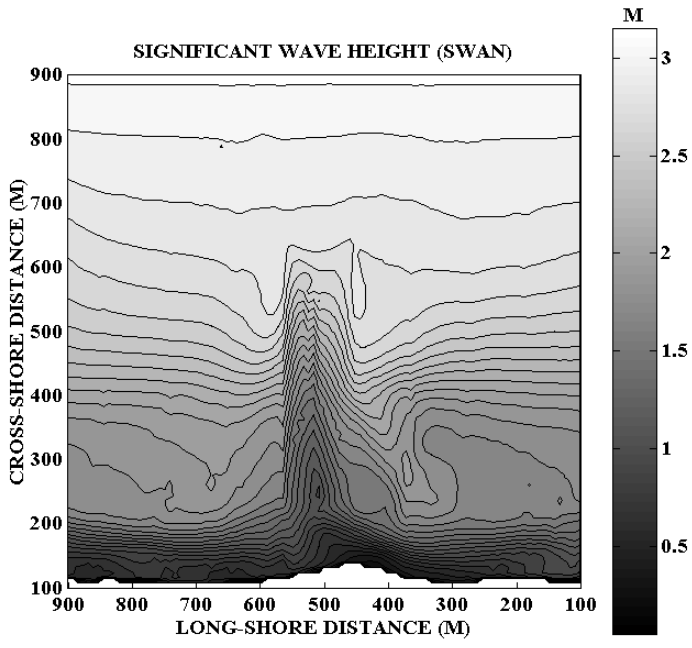

(Top Panel)

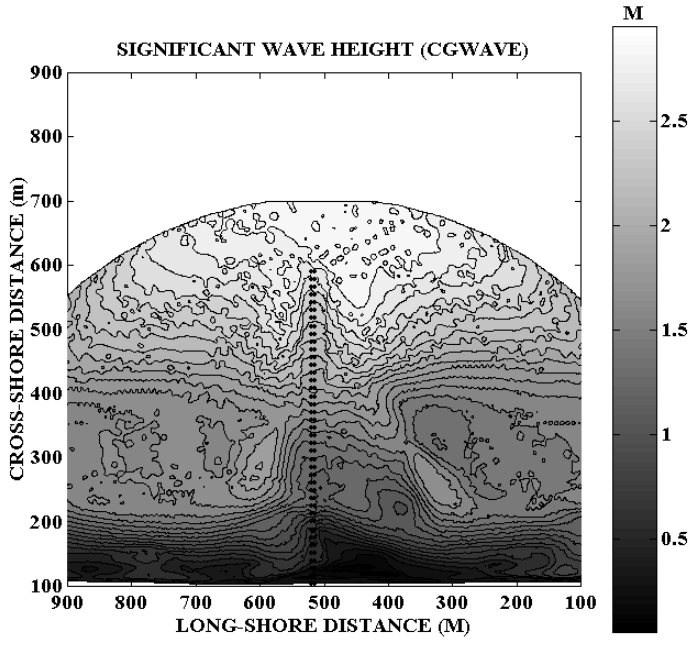

(Bottom Panel)

Fig. 6. Significant wave heights computed by SWAN (top panel) and CGWAVE (bottom panel) for the May 1998 simulations.

the observed changes in the significant wave heights very well for the three storm events.

In addition to the "all-on" SWAN runs; six additional SWAN runs were made for each storm event, by turning off the physical mechanisms one at a time. This allows one to determine the significance of each mechanism on the wave transformation near FRF. Of these runs, the computed significant wave heights and mean wave periods (Table 2) deviate from the "all-on" runs and from the observations when refraction and bottom-induced breaking are turned off, indicating that these are the two most significant mechanisms affecting wave evolution. The other physical mechanisms, viz. wind, bottom friction, white-capping, and triad wave-wave interaction showed little significance. This validates, to a large extent, the suitability of CGWAVE, in which the effects of wind, white-capping, and wave-wave interactions are absent, for simulating these cases.

Figure 6 (bottom panel) shows a contour plot of the significant wave heights computed with CGWAVE for the 1998 storm event. From Table 3 and Fig. 7 (bottom panel), it can be seen that at gauge G625, CGWAVE results are, on average, smaller than the observations (and the SWAN results); the discrepancy is much less at gauge G641. Additional CGWAVE runs were made with the breaking turned off to quantify

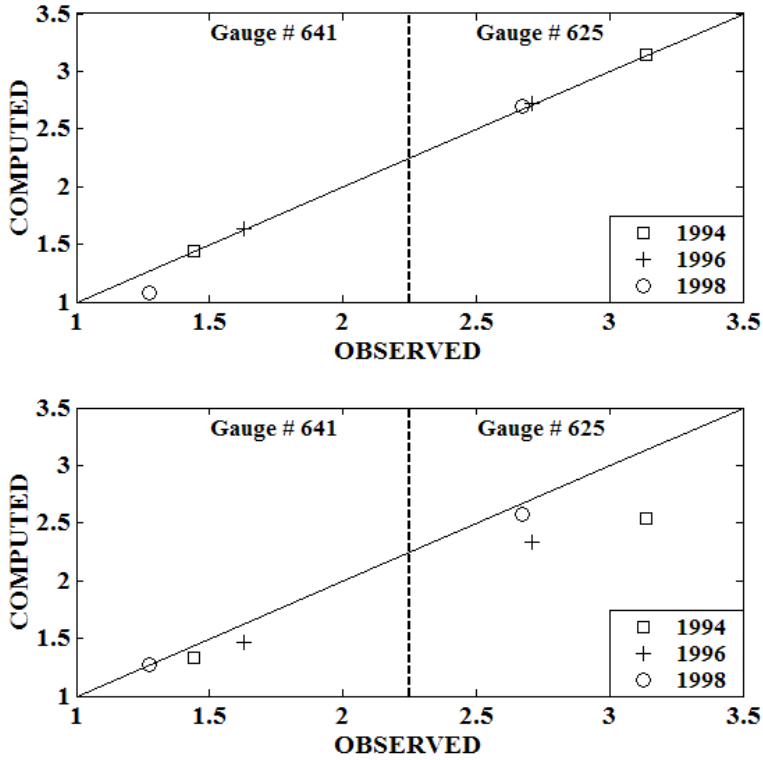

Fig. 7. Significant wave height comparisons for SWAN (top panel) and CGWAVE (bottom panel) for the three storm events.

Table 3. CGWAVE-computed significant wave height (Hs) for three storm events, with and without breaking.

	Date:	Nov. 18, 1994	Sep. 06, 1996	May 13, 1998
	Time:	04:00–06:16	01:00–03:16	13:00–15:16
Physics	Gage #	Hs (m)	Hs (m)	Hs (m)
With Breaking	625	2.540	2.340	2.580
	641	1.388	1.468	1.276
W/O Breaking	625	4.080	2.440	3.020
	641	2.640	2.580	1.834

the significance of the breaking mechanism. The results (Table 3) showed that the bottom-induced breaking is indeed significant. While it is not possible to turn off refraction in CGWAVE (since it is inherent in the "combined refraction-diffraction" equation), the example in Fig. 5 (top panel) clearly shows its importance. Thus the results of the two models are compatible insofar as the identification of the dominant mechanisms for these simulations is concerned.

For comparing the performance of the two models, instead of relying only on the two gauge locations, we also examined the significant wave heights obtained by the two models along three cross-shore sections (Fig. 8). The sections were taken along the pier line and to the right and left of the pier at cross-shore coordinates (shown in Fig. 1) equal to 275 m (Right Section) and 775 m (Left Section). Figure 8 shows that for the 1994 and 1996 events, significant wave heights computed by CGWAVE were always less than those computed by SWAN along all three sections. For the 1998 storm event, CGWAVE results along the pier line were closer to SWAN results but along the two other sections, the significant wave heights obtained with CGWAVE were again smaller. Despite the fact that CGWAVE results were quantitatively lower, the two models show qualitatively similar behavior along the three sections for the three events. The two models also behaved in the same way when the breaking was turned off for the three storms, as can be seen in Fig. 9. For both models, the onset of breaking is found to occur far offshore and not only in shallow waters. (Note that for the 1996 case, for the cross-shore distance between 700 m and 400 m, SWAN results with breaking are higher than CGWAVE results with and without breaking. This is due to the fact that in CGWAVE the waves at 700 m are already low such that the waves are not significantly affected by breaking. This is not the case for the 1994 and 1998 events mainly because of the differences in both the bathymetry and the input wave characteristics.)

In addition to the numerics (relatively coarse finite difference grids versus high-resolution finite element grids), the differences in the model results noted in the above paragraph may be attributed to the input conditions and the wave physics modeled. To examine the effect of the former (i.e. the number of spectral components), the reduced spectra were used (as done for CGWAVE) to force

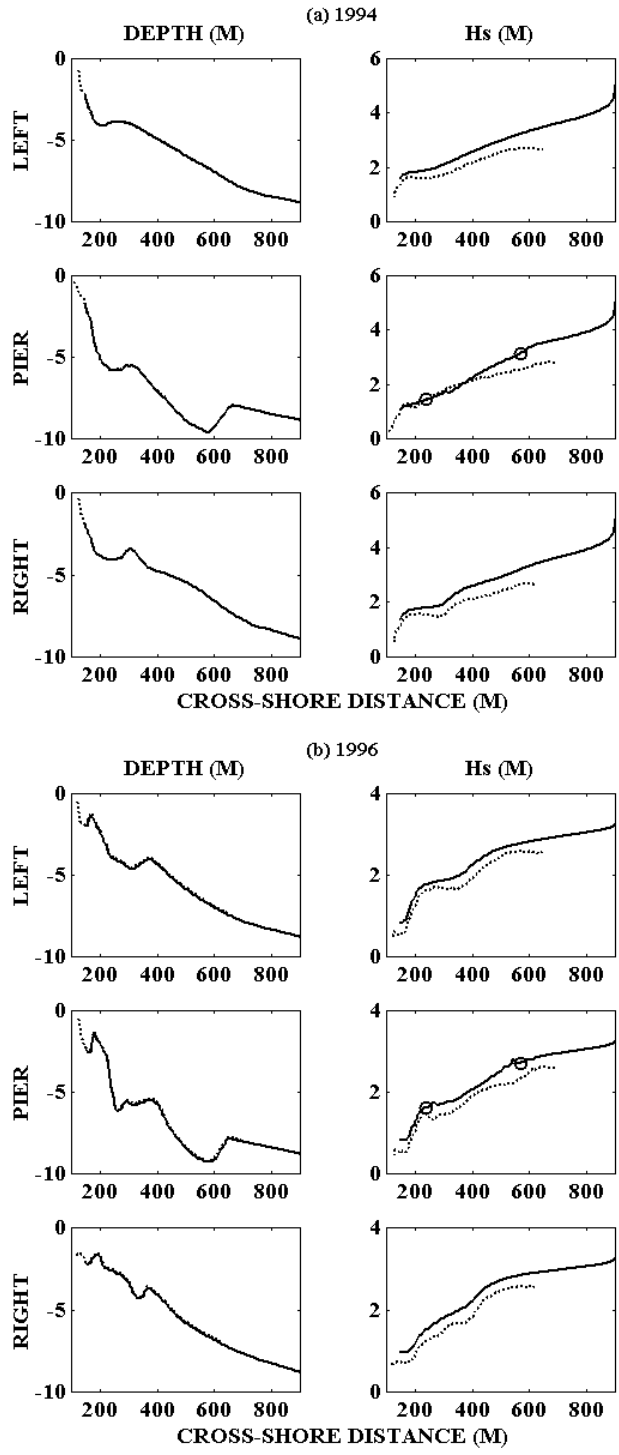

Fig. 8. Water depth profile and significant wave heights (Hs) obtained with SWAN (solid lines) and CGWAVE (dashed lines) along three different cross-shore sections for the (a) 1994, (b) 1996, and (c) 1998 simulations. Circles (o) represent observed significant wave heights at two gauge locations.

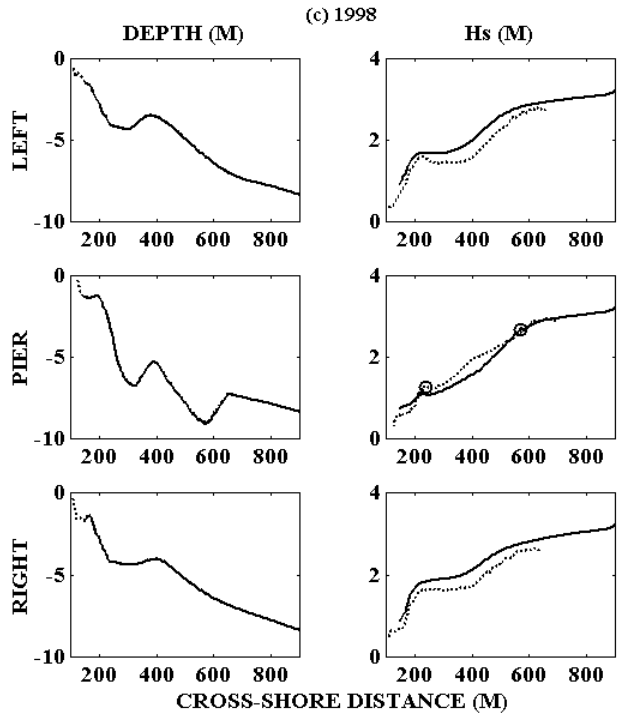

Fig. 8 (*Continued*)

SWAN for the three storm events. For both 1998 and 1996 storm events there were insignificant changes in the results. The 1994 case showed a slight change in the significant wave height (of the order of about 0.3 m at the "G625" and "G641" wave gauges). There were no changes in the SWAN-computed peak wave periods. Turning to wave physics, refraction was seen to be properly modelled (Fig. 5) by both models. (In any case it is not possible to "turn off" refraction in CGWAVE). The similarity of the overall results and the discussion provided earlier preclude the absence of pier-induced diffraction in SWAN and the absence of wind generation in CGWAVE as possible sources of discrepancy. The good performance shown by SWAN for the three storm events and also the consistency in the results of CGWAVE and SWAN along the research pier line indicate that bathymetric and structural (piling-induced) diffraction (which is absent in SWAN) is not particularly significant for the wave periods investigated. The discrepancies may hence be attributed to wave breaking and nonlinear interactions.

Wave breaking is simulated in the two models in different ways. CGWAVE uses the Dally *et al.* (1985) formulation without tuning the stable wave factor and wave decay factor used therein, while SWAN uses the Battjes and Janssen (1978) formulation. For examining the effect of these formulations, wave propagation over the bar-trough bathymetry (Fig. 10) used by Booij *et al.* (1999) was modelled with a simple, one-dimensional version of CGWAVE. The results (Fig. 10) and other

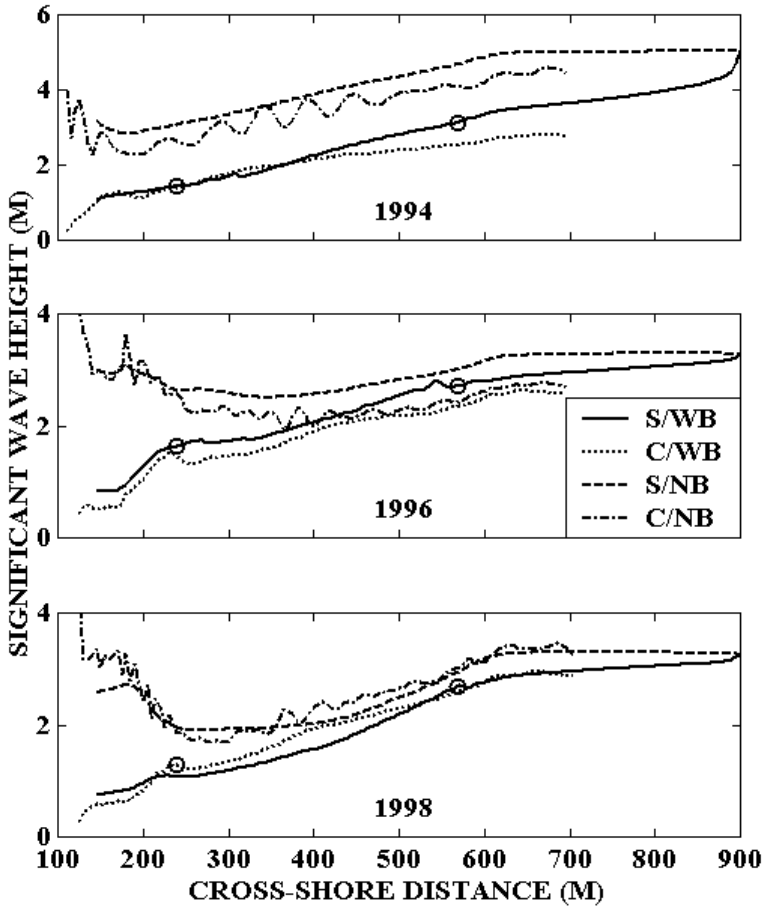

Fig. 9. SWAN (S) and CGWAVE (C) computed significant wave height, with and without breaking (WB and NB), along the pier line section for the three storm events. Circles (o) represent observed significant wave heights at two gauge locations.

tests described by Zhao *et al.* (2001) suggest that the Dally *et al.* (1985) breaking formulation (denoted by DDD in Fig. 10) underestimates the observed wave heights somewhat, compared with the laboratory data and the Battjes and Janssen (1978) formulation (denoted by BJ). (Of course, the values for the two parameters (stable wave factor and wave decay factor) may be adjusted according to the bottom slope, but that is difficult for field applications.) Clearly, the treatment of breaking is a dominant factor influencing the discrepancy between the models. However, as described in Sec. 4.2, breaking is linked to wave-wave interactions as well.

4.2. *Qualitative model performance*

Chen *et al.* (1997), Elgar *et al.* (1997), and Herbers *et al.* (2000) suggested that nonlinear interactions in the FRF surf zone transfer energy to higher frequencies from where it is rapidly dissipated by bottom-induced breaking. At the two wave

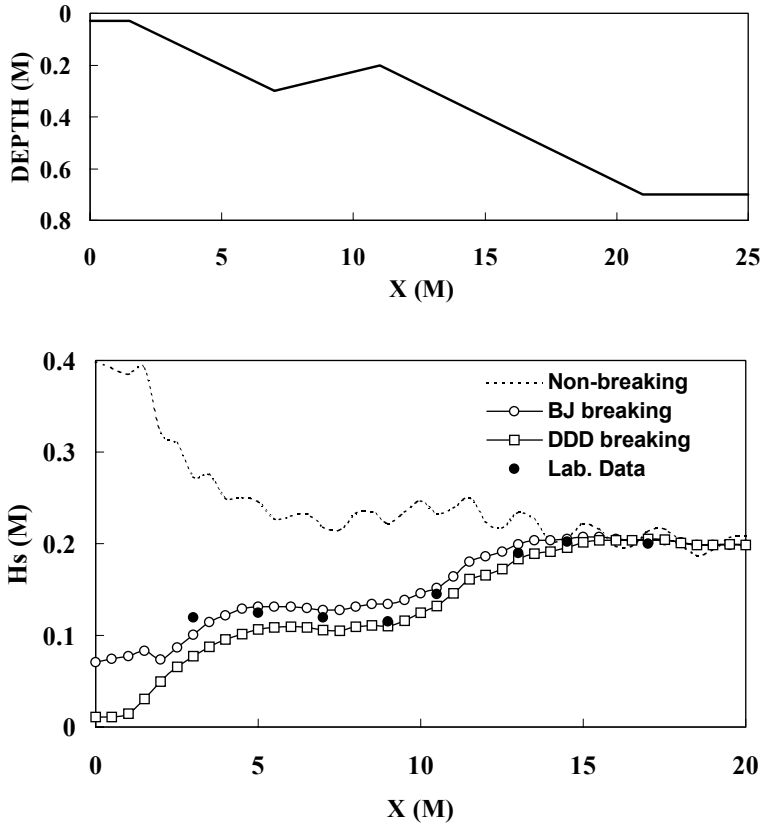

Fig. 10. Water depth profile (top panel) and CGWAVE-computed significant wave height comparison (bottom panel).

gauge locations, however, we have noted that the effect of the wave-wave interactions was insignificant (Table 2). In light of the suggestions by Chen *et al.* (1997), Elgar *et al.* (1997), and Herbers *et al.* (2000), the effect of wave-wave interactions over the entire domain was investigated. Figure 11 shows the values obtained by subtracting the significant wave heights of the "all-on" run from the significant wave heights of the "triad-off" run for the 1998 simulation using SWAN. Maximum positive values are found to occur along the surf zone that extends in the cross-shore direction to a distance of about 100 m offshore. In these areas, the "triad-off" wave heights are larger than the "all-on" wave heights, suggesting that breaking has less of an effect when the interactions are absent. This is confirmed by examining the spectral characters for the "all-on" and the "triad-off" runs for theses areas; see Fig. 12. For each simulation, the triad interactions are seen to transfer energy from the low frequency part of the spectrum to the high frequency part. Thus a greater amount of energy is available for dissipation in the high frequency waves (which are physically more susceptible to breaking), leading to smaller wave heights. These numerical

results are consistent with the suggestions of Chen *et al.* (1997), Elgar *et al.* (1997) and Herbers *et al.* (2000).

While the effect of wave-wave interactions on the overall SWAN results is somewhat small at the gauges, as seen earlier, we have just seen that it influences wave breaking in shallow areas. Due to the difference in the breaking formulation, the discrepancy between the results of the two models as one approaches the nearshore areas could be expected to increase (based on Fig. 10). However the differences diminish (Fig. 8), because of the role of wave-wave interactions in this area, which is to enhance the effect of breaking in SWAN. In a sense, the combination of wave-wave interactions and breaking with the Battjes and Janssen (1978) formulation (in SWAN) has the same effect as breaking with the untuned Dally *et al.* (1985) formulation (in CGWAVE) in shallow areas. Further offshore, the larger wave heights seen along the transects in Fig. 8 for SWAN may be attributed to the effect of wave-wave interactions: in this area, the effect of wave-wave interactions is to create an energy distribution such that breaking effects are smaller, hence enhancing the wave heights (based on Fig. 11).

By examining the field data from FRF, Herbers *et al.* (1999) suggested that wave breaking over the sand bar causes significant scattering of wave energy and enhanced

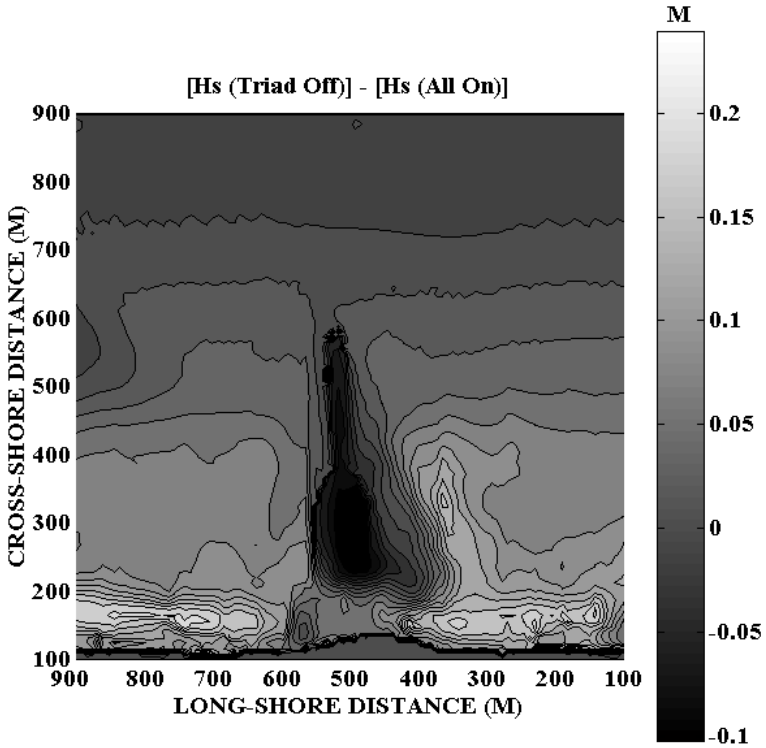

Fig. 11. Difference between "all on" significant wave heights and "triad off" significant wave heights obtained from SWAN for the May 1998 simulation.

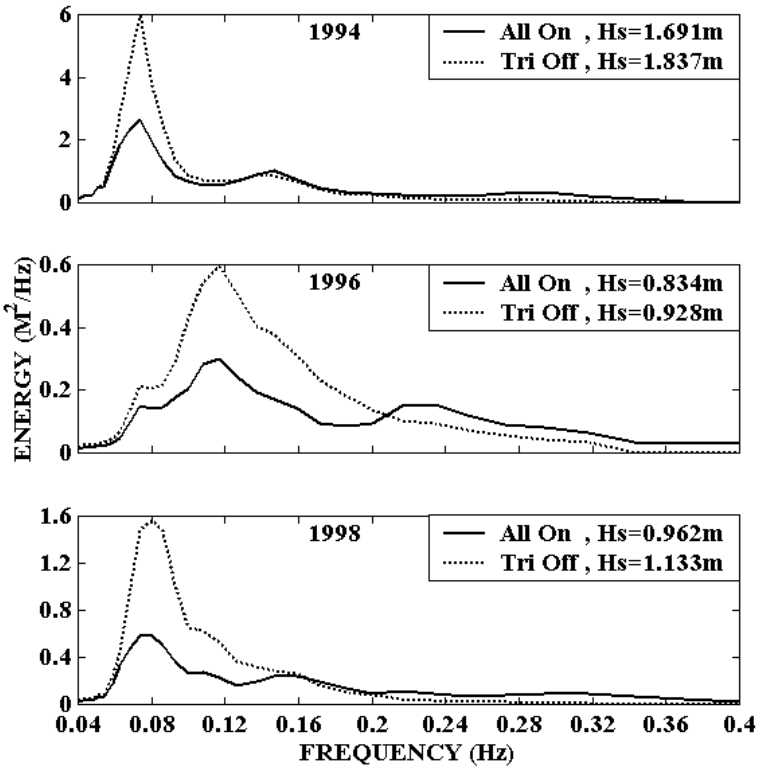

Fig. 12. Spectra and significant wave heights (Hs) obtained using SWAN with all physical mechanisms turned on (All On) and with the triad wave-wave interaction turned off (Tri Off) at nearshore locatiions.

directional spreading. Their estimates of directional spreading along FRF cross-shore transects are shown in Fig. 13; these results are based on data collected when the nearshore bar was present. Since the location of the nearshore bar frequently changes (Gallagher *et al.* (1998) and Fig. 14) and the periods associated with our model simulations and the field measurement program of Herbers *et al.* (1999) are different, we may view Fig. 13 in a representative sense and use it only for an approximate comparison. Figure 14 shows the directional spreading calculated by SWAN along cross-shore transects for the three events. In general, the model results are similar to the estimates of Herbers *et al.* (1999) in that the wave directional spreading is enhanced in the vicinity of the nearshore sand bar. The similarity is pronounced when the bathymetry is similar (compare Fig. 14(c) with data for 30 September in Fig. 13).

In Fig. 14, we also show directional spreading calculated by SWAN with wave breaking turned off. Breaking is seen to enhance the directional spreading in the nearshore areas, which agrees with the suggestion of Herbers *et al.* (1999). Again the greatest enhancement is seen for the 1998 case. For the other two cases, however, the effect appears to be somewhat minimal. This is probably because the breaking

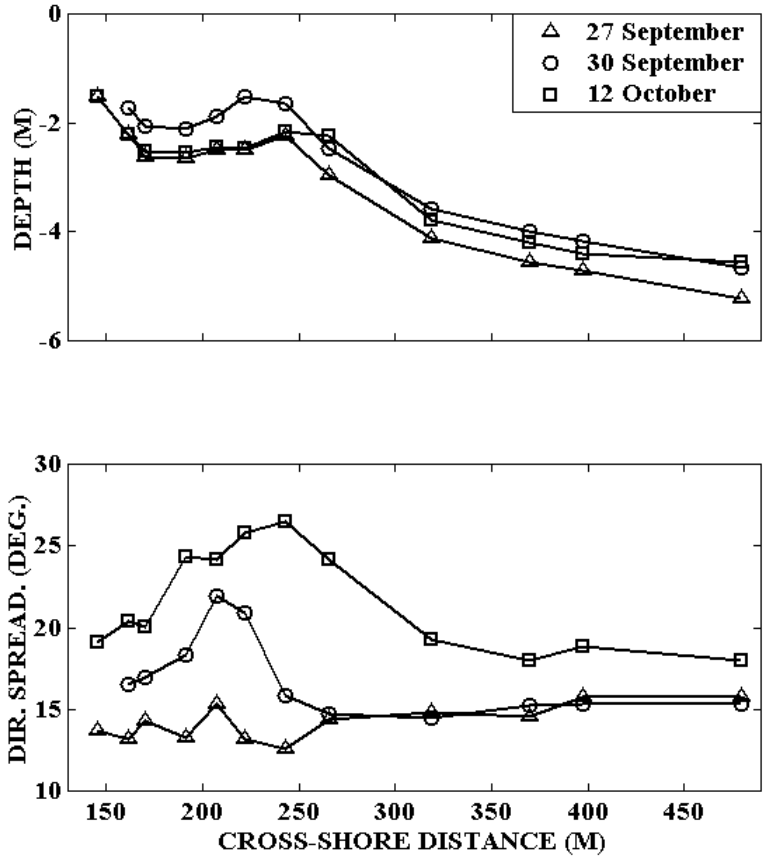

Fig. 13. Water depth profiles (top panel) and the wave directional spreading (bottom panel) observed along cross-shore transects for three storm events in 1994 (after Herbers *et al.* 1999).

mechanism in SWAN is not strongly dependent on wave direction (and also of course, because the bathymetries are different). Overall, the results from SWAN tend to confirm the observations of Herbers *et al.* (1999).

Miller *et al.* (1983) investigated the effect on the waves of the deep bathymetric trough near the offshore end of FRF research pier. Their statistical comparison of measurements at two locations (gauge G625 at the end of the pier and another gauge (GM83) located about 300 m to the northeast from it, see Fig. 1) showed that during normal wave conditions, the wave parameters were identical at the two locations; however, during storm conditions, the high waves were usually about 10 to 15% lower at gauge G625. CGWAVE and SWAN results were investigated at these two locations for the three storm events (Table 4). The comparisons showed that the modelled waves were lower at wave gauge G625 by approximately 10% (on average). Thus, the modelled results are consistent with the observations of Miller *et al.* (1983).

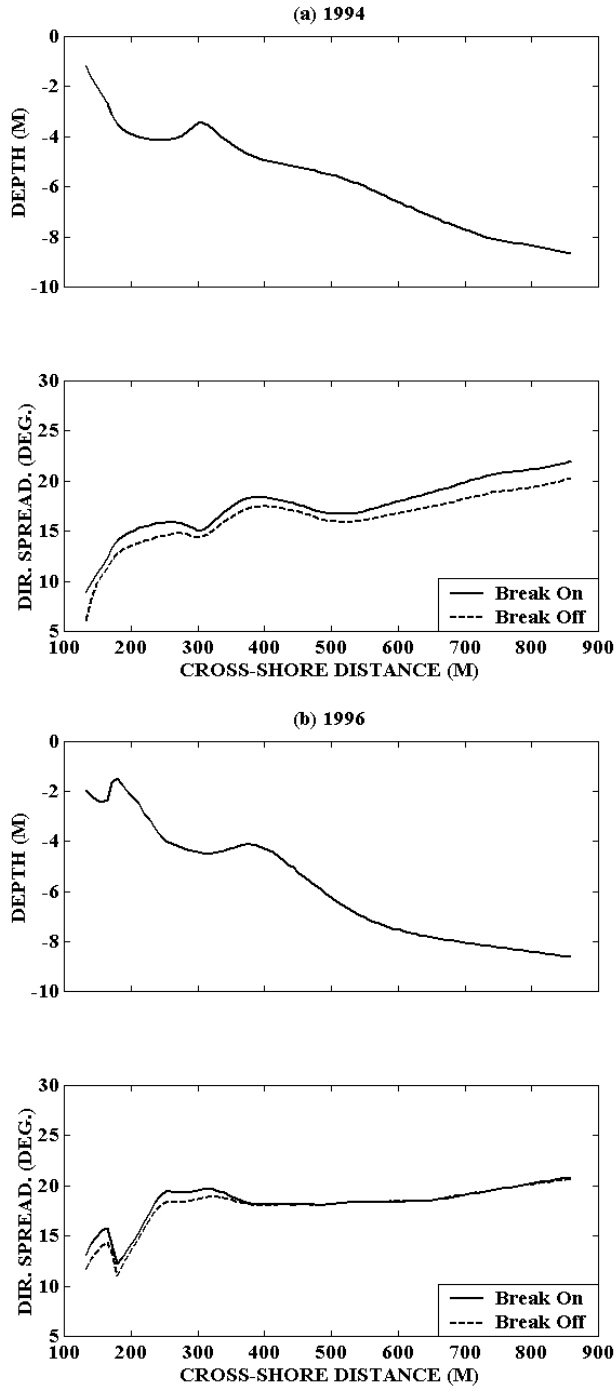

Fig. 14. Water depth profiles (top panel) and the SWAN-Computed wave directional spreading (bottom panel) with breaking (Break On) and with no breaking (Break Off), along a cross-shore transect for the (a) 1994, (b) 1996, and (c) 1998 simulations.

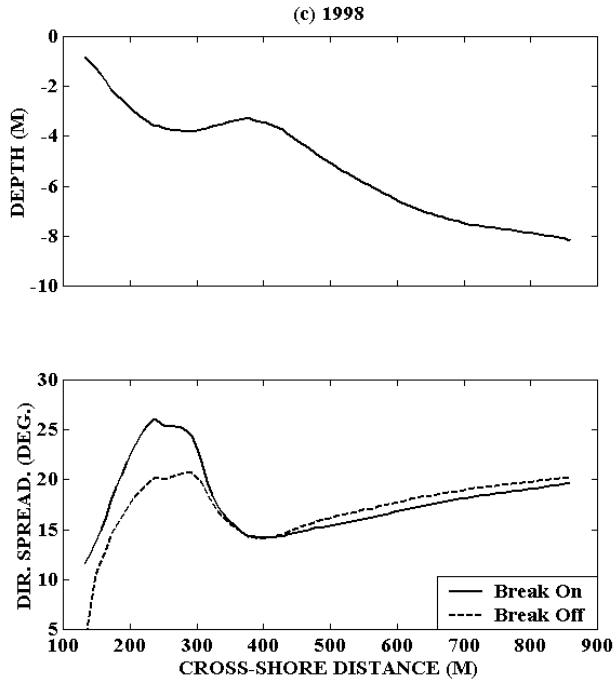

Fig. 14 (*Continued*)

Table 4. Significant wave height comparison between wave gauge G625 and near the location of the wave gauge (GM83) used by Miller *et al.* (1983).

Date	SWAN			CGWAVE		
	G625	GM83	%	G625	GM83	%
Nov. 18, 1994	3.143	3.593	12.52	2.541	2.754	07.73
Sep. 06, 1996	2.717	2.972	08.60	2.340	2.621	10.72
May 13, 1998	2.692	2.958	09.00	2.580	2.880	10.42
Average			10.04			09.63

4.3. *Effect of the pilings*

The present modeling study also enables one to address the issue of the pier legs on measurements made at the highly-used Field Research Facility. In a recent paper, Elgar *et al.* (2001) presented some data obtained from the north of the pier in the region bounded approximately between $x \approx 700$ m and $x \approx 900$ on (long-shore coordinates, see Fig. 1) and $y \approx 150$ m and $y \approx 500$ m (cross-shore coordinates). Data for two cross-shore transects are shown in Fig. 15 for waves approaching the pier from the southeast during a low-wave event in 1997. Using a simple refraction model, Elgar *et al.* (2001) attributed the observed reduction in the wave heights in the cross-shore direction in the immediate shadow of the piers (e.g. $x = 703$ m) to a

30–50% "wave blocking" effect induced by the pier legs. Further away from the pier (e.g. $x = 905$ m), there is no such reduction because wave reaching this area do not traverse through the pier legs. CGWAVE can explicitly include internal boundaries in a non-empirical manner. It solves the governing equations as boundary value problem with an assigned reflection coefficient for the piles. Therefore, it was used to perform two dissipation-less simulations with and without the pier legs being accommodated in the model domain. Although the pier legs are not accommodated in SWAN, a simulation using SWAN has also been made with wind, nonlinear wave-wave interactions and all dissipation mechanism turned off. For grid generation and input conditions for the two models, we followed the same modeling schemes presented earlier (Sec. 3) for the three storm events (i.e. grid generation, spectral discretization, etc.). It must be noted here that our model domains are completely different in size from the domain used by Elgar *et al.* (2001) and so are the locations where the input conditions are provided to the model. To obtain input conditions, Elgar *et al.* (2001) performed back-refraction of the frequency-directional spectra observed at the 5 m water depth to estimate input wave conditions at 6.5 m depth. For the sake of consistency in the inter-model comparisons, the energy contained in

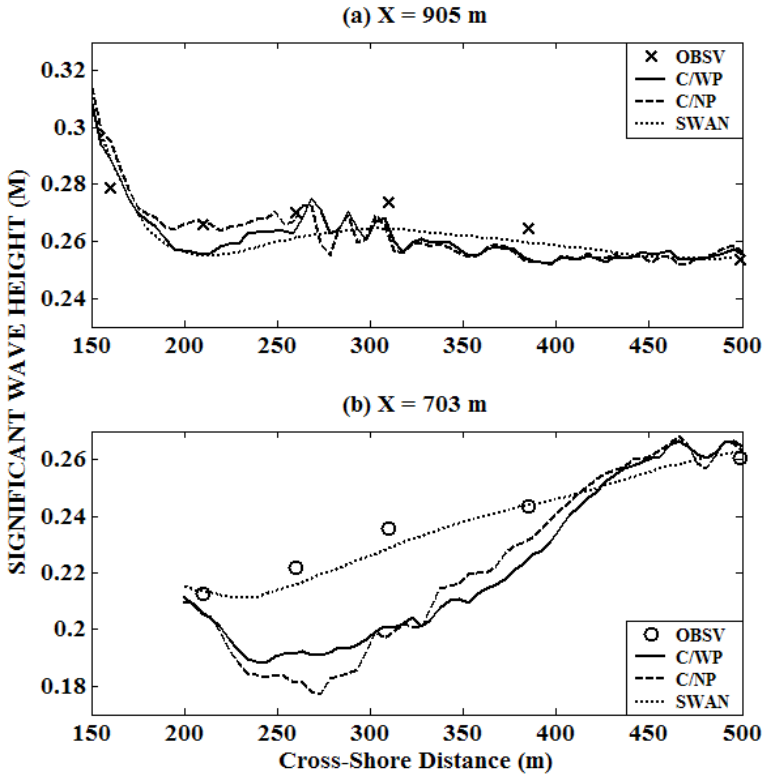

Fig. 15. Observations (OBSV) of Elgar *et al.* (2001) and modelled significant wave height along (a) $x = 905$ m and (b) $x = 703$ m for the 1997 case. CGWAVE results with pilings (CWP) and with no pilings (CNP); and SWAN results (SWAN).

the input spectrum from the 8 m array (8.5 m water depth) was adjusted in order to reproduce the farthest observations of Elgar *et al.* (2001) (i.e. at $y = 500$ m).

In Fig. 15, the significant wave heights obtained using CGWAVE with and without the pier legs (denoted by CWP and CNP) along the two cross-shore transects ($x = 703$ m and $x = 905$ m) are shown. [The oscillations in the wave heights produced by CGWAVE are due to diffractive effects, typically seen near areas of complex bathymetry such as shoals and trenches (e.g. Bondzie and Panchang, 1993).] Although CGWAVE results show some underestimation in comparison with the observations (along the $x = 703$ m transect), the observed increasing and decreasing trends are still obtained. The reasonable agreement between the results with and without the pilings suggests that the effect of the pilings is very minimal and cannot account for the 30–50% blocking suggested by Elgar *et al.* (2001). This suggests that the observed reduction in the wave heights is probably an effect of the deep bathymetric trench that is located under the pier. One way to confirm this suggestion is by using SWAN (which does not accommodate the pilings) to simulate this case. Figure 15 shows the significant wave heights obtained using SWAN for this case. The comparison between SWAN results and the observations along the two cross-shore sections showed good agreement. Furthermore, the comparison between SWAN computed and observed spectra at three different gauge locations, Fig. 16, showed reasonable agreement. This indicates that the pier legs (not included

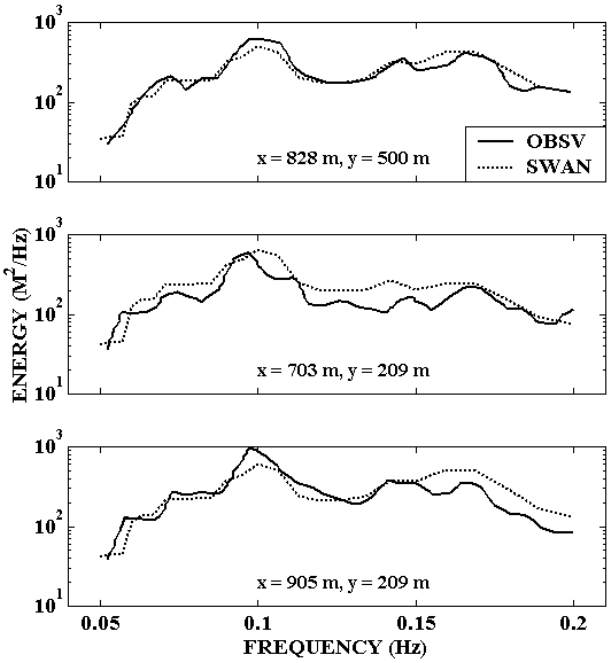

Fig. 16. Elgar *et al.* (2001) Observed (OBSV) and SWAN-computed (SWAN) wave energy spectra at three gauge locations for the 1997 case.

in SWAN domain) have an insignificant effect on the waves for the investigated conditions. However, this may not always be the case, since the wave blocking and diffraction/reflection by circular objects (e.g. pier legs) are in fact functions of the wave conditions. The apparent wave height reduction in the immediate shadow of the pier for the case presented here is hence attributable to the deep bathymetric trench located under the pier.

5. Concluding Remarks

It is often necessary to implement wave models on coastal domains where there are insufficient data for validation. Results may have to be accepted at face value (without tuning). This is difficult from the user's viewpoint; for example, see Thieler *et al.* (2000) who suggest that several models may demonstrate poor performance in the field. It is therefore important to demonstrate that the models provide reasonable predictions using whatever data are available.

In this paper, we have demonstrated that CGWAVE and SWAN provide fairly accurate simulations of three events modelled at the FRF, Duck (North Carolina). Although the two models are intended for different types of applications as a consequence of differing physics, turning various physical mechanisms on and off allowed an inter-comparison. It was demonstrated that the underestimation of wave heights by CGWAVE was possibly due to the absence of wave-wave interactions and the use of Dally *et al.* (1985) breaking formulation with unadjusted wave decay factors. Inclusion of wind generation on length scale of about 1 km (the approximate size of the domains modelled) has little effect. SWAN was able to qualitatively confirm observational findings of other researchers regarding wave breaking, triad wave-wave interactions, and wave directional spreading at this site.

In a recent study, Elgar *et al.* (2001) have suggested including the effects of the pier legs through an empirical wave blocking mechanism. Here we have used CGWAVE, which includes structural and bathymetric diffraction, to show that the pier legs have little effect for the case examined. Further, the trends observed by Elgar *et al.* (2001) in the shadow of the pier and further away from it were replicated by CGWAVE and also by SWAN, which does not accommodate the pier legs. While the similarity of the results of SWAN and CGWAVE indicated that bathymetric and structural diffraction effects were not significant in the dissipative simulations, there is no guarantee that this will always be the case for all incident wave conditions; e.g. differences can certainly be expected for narrow peaked spectra or swell conditions (Bondzie and Panchang, 1993). Here too, variability in the wave field is found to be enhanced for non-breaking waves (e.g. Figs. 9 and 15). The analysis and results presented here show that when the modelled physics are commensurated with what is occurring in the field, both models provide fairly reasonable and compatible predictions.

Acknowledgments

Partial support for this work was provided by the Office of Naval Research, the Maine Sea Grant Program, and the National Sea Grant Office. Assistance rendered by Karl Schlenker, Wei Chen, and Luizhi Zhao is gratefully acknowledged. Comments provided by three anonymous reviewers were instrumental in improving this paper. Permission to publish this paper was granted by the Chief, US Army Corps of Engineers.

References

Battjes, J. A. and Jenssen J. (1978). Energy loss and set-up due to breaking of random waves, *Proc. 16th Int. Conf. Coastal Engineering*, ASCE, 569–587.

Bondzie, C. and Panchang V. G. (1993). Effects of bathymetric complexities and wind generation in a coastal wave propagation model, *Coastal Eng.* **21**: 333–336.

Booij, N., Holthuijsen, L. H. and Ris R. C. (1996). The "SWAN" wave model for shallow water, *Proc. 25th Int. Conf. Coastal Engineering*, ASCE, 668–676.

Booij, N., Holthuijsen, L. H., Doorn N. and Kieftenburg, A. T. M. M. (1997). Diffraction in a spectral wave model, *Ocean Wave Measurements and Analysis, Proc. 3rd Int. Sympos., Waves'97*, ASCE, 243–255.

Booij, N., Ris, R. C. and Holthuijsen, L. H. (1999). A third-generation wave model for coastal regions, 1, model description and validation, *J. Geophys. Res.* **104**, C4, 7649–7666.

Bova, S. W., Breshears, C. P., Cuicchi, C., Demirbilek, Z. and Gabb, H. A. (2000). "Dual level parallel analysis of harbor wave response using MPI and OpenMPI. *Int. J. High Performance Computing Appl.* **14**, 1, 49–64.

Chawla, A., Ozkan-Haller, H. T. and Kirby J. T. (1998). Spectral model for wave transformation and breaking over irregular bathymetry, *J. Waterway, Port, Coast, Ocean. Eng.* **124**: 843–855.

Chen, Y., Guza, R. T. and Elgar, S. (1997). Modeling spectra of breaking surface waves in shallow water, *J. Geophys. Res.* **102**, C11, 25035–25046.

Dally, W. R., Dean, R. G. and Dalrymple, R. A. (1985). Wave height variation across beaches of arbitrary profile, *J. Geophys. Res.* **90**, C6, 11917–11927.

Demirbilek, Z. and Panchang, V. G. (1998). CGWAVE: A coastal surface water wave model of the mild slope equation, Technical Report CHL-98-26, US Army Corps of Engineers, Waterways Experiment Station, Vicksburg, MS 39180.

Elgar, S., Guza, R. T., Herbers, T. H. C., Raubenheimer, B. and Gallagher E. L. (1997). Spectral evolution of shoaling and breaking waves on a barred beach, *J. Geophys. Res.* **102**, C7, 15797–15805.

Elgar, S., Guza, R. T., O'Reilly, W. C. O., Raubenheimer, B. and Herbers, T. H. C. (2001). Wave energy an direction observed near a pier, *J. Waterway, Port, Coast, Ocean. Eng.* **127**, 1, 1–6.

Gallagher, E. L., Elgar, S. and Guza, R. T. (1998). Observation of sand bar evolution on a natural beach, *J. Geophys. Res.* 103, C2, 3203-3215.

Herbers, T. H. C., Elgar, S. and Guza, R. T. (1999). Directional spreading of waves nearshore, *J. Geophys. Res.* **104**, C4, 7683–7693.

Herbers, T. H. C., Russnogle, N. R. and Elgar, S. (2000). Spectral energy balance of breaking waves within the surf zone, *J. Phys. Oceaogr.* **30**: 2723–2737.

Howd, P. A. and Birkemeier, W. A. (1987). Storm-induce changes during duck85, *Coastal Sediments'87*, Waterways Division/ ASCE, New Orleans, LA, 834–847.

Kaihatu, J. and Kirby J. T. (1995). Nonlinear transformation of waves in finite water depth, *Phys. Fluids.* **7**, 8, 1903–1914.

Komen, G. J., Cavaleri, L., Donlean, M., Hasselmann, K., Hasselmann, S. and Janssen, P. A. E. M. (1995), *Dynamics and Modeling of Ocean Waves*, Cambridge University Press, Cambridge, UK.

Mei, C. C. (1983). *The Applied Dynamics of Ocean Surface Waves*, Wiley, New York.

Miller, H. C., Birkemeier, W. A. and Dewall, A. E. (1983). Effects of CERC research pier on nearshore processes, *Coastal Structures '83*, US Army Coastal Engineering Research Center, 769–784.

Panchang, V. G., Ge, W., Pearce, B. R. and Briggs, M. J. (1990). Numerical simulation of irregular wave propagation over a shoal, *J. Waterway, Port, Coast, Ocean. Eng.* **116**, 3, 324–340.

Panchang, V. G., Xu, B. and Demirbilek, Z. (1998). Wave prediction models for coastal engineering applications, Ch. 4 — Developments in Offshore Engineering, ed. J. B. Herbich, Gulf Publishing, Houston, TX, 163–194.

Panchang, V. G., Chen, W., Xu, B., Schlenker, K., Demirbilek, Z. and Okihiro, M. (2000). Exterior bathymetric effects in elliptic harbor wave models, *J. Waterway, Port, Coast, Ocean. Eng.* **126**, 2, 71–78.

Panchang, V. G. and Demirbilek, Z. (2001). Simulation of waves in harbors using two dimensional elliptic equation models, *Advances in Coastal & Ocean Engineering* **7**: 125–162, World Scientific, Singapore.

Panchang, V. G. and Demirbilek, Z. (2002). Simulation of waves in two harbors: Validation of a state-of-the-art model, *Proc. HYDRO 2002*, Indian Institute of Technology, Bombay, December 2002, pp. 210–214.

Pearce, B. R. and Panchang, V. G. (1985). A method for the investigation of steady state wave spectra in bays, *J. Waterway, Port, Coast, Ocean. Eng.* **111**, 4, 629–644.

Ris, R. C. (1997). Spectral modeling of wind waves in coastal areas, *Commun. Hydraulics and Geotechnical Engineering* Report No. 97–4, Delft University of Technology.

Ris, R. C., Booij, N., Holthuijsen, L. H., Padilla-Hernandez, R. and Haagsma, IJ. G. (1998). SWAN cycle 2 users' manual, For SWAN version 30.75, Unauthorized Electronic Version, Delft University of Technology.

Ris, R. C., Holthuijsen, L. H. and Booij, N. (1999). A third-generation wave model for coastal regions, 2, verification, *J. Geophys. Res.* **104**, C4, 7667–7681.

Rogers, W. E., J. M. Kaihatu, H. A. H. Petit, N. Booij and L. H. Holthuijsen (2002). Diffusion reduction in an arbitrary scale third generation wind wave model, *Ocean Eng.* pp. 1357–1390.

Siddabathula, M. and Panchang V. G. (1996). Quality control of geosat wave data for engineering applications, *Proc. 25th Int. Conf. Coast. Eng.*, Orlando, September 1996, pp. 81–94.

Tang, Y. and Ouellet Y. (1997). A new kind of nonlinear mild-slope equation for combined refraction-diffraction of multifrequency waves, *Coastal Eng.* **31**: 3–36.

Thieler, E. R., Pilkey, O. H., Young, R. S., Bush, D. M. and Chai, F. (2000). The use of mathematical models to predict beach behavior for coastal engineering: A critical review, *J. Coastal Res.* **16**, 1, 48–70.

Thompson, E. F., Chen, H. S. and Hadley, L. L. (1996). Validation of numerical model for wind waves and swell in harbors, *J. Waterway, Port, Coast, Ocean. Eng.* **122**, 5, 245–256.

Tolman, H. L. (1989). The numerical model WAVEWATCH: A third generation model for the hindcasting of wind waves on tides in shelf seas, *Commun. Hydraulic and Geotechnical Eng.*, Delft University of Technology, ISSN 0169–6548, Report No. 89–2.

Zhao, L., Panchang, V. G., Chen, W., Demirbilek, Z. and Chhabbra, N. (2001). Simulation of breaking effects in a two-dimensional harbor wave prediction model, *Coastal Eng.* **42**, 4, 359–373.

Zundel, A. K., Fugal, A. L., Jones, N. L. and Demirbilek, Z. (1998). Automatic definition of two-dimensional coastal finite element domains, *Hydroinformatics'98*, *Proc. 3rd Int. Conf. Hydroinformatics*, ed. V. Babovic and L. C. Larsen, A. A. Balkema, Rotterdam, 693–700.